

Supplementary Information

Lanthanide-Organic Crystalline Framework Material Encapsulated by 1,3,6,8-tetrakis (p-benzoic acid) pyrene: Selective Sensing on Fe³⁺, Cr₂O₇²⁻ and Colchicine and White-light Emission

Jin Xiao Li^a, Qing Lin Guan^a, Yu Wang^a, Zi Xin You^a,

Yong Heng Xing^{a}, Feng Ying Bai^{a*}, Li Xian Sun^b*

^a College of Chemistry and Chemical Engineering, Liaoning Normal University,
Huanghe Road 850#, Dalian 116029, P. R. China

^b Guangxi Key Laboratory of Information Materials, Guilin University of Electronic
Technology, Guilin 541004, P. R. China

* Corresponding author. E-mail address: xingyongheng2000@163.com (Y. H. Xing);
baifengying2003@163.com (F. Y. Bai)

Supplementary Index

Synthetic process of the ligand H₂MCTCA	1
Figure S1. The ¹ H-NMR spectrum of the ligand H ₂ MCTCA.....	1
Figure S2. The ¹³ C-NMR spectrum of the ligand H ₂ MCTCA.....	2
Figure S3. The HRMS spectrum of the ligand H ₂ MCTCA	2
Synthetic process of the H₄TBAPy	2
Figure S4. The ¹ H-NMR spectrum of H ₄ TBAPy ligand in <i>d</i> ₆ -DMSO	3
Figure S5 PXRD patterns of the Eu-MCTCA and Eu-MCTCA@H ₄ TBAPy.....	4
Figure S6 Appearance of Eu-MCTCA and Eu-MCTCA@H ₄ TBAPy.....	4
Figure S7 IR spectra of the Eu-MCTCA and Eu-MCTCA@H ₄ TBAPy.....	4
Figure S8 UV-vis spectra of the Eu-MCTCA and Eu-MCTCA@H ₄ TBAPy	5
Figure S9 The solid-state luminescent spectrum for H ₂ MCTCA Eu-MCTCA and Eu-MCTCA@H ₄ TBAPy at room temperature	5
Figure S10 Fluorescence spectra of supernatant of H ₄ TBAPy and Eu-MCTCA@H ₄ TBAPy after ultrasonic treatment	6
Figure S11 CIE chromaticity diagrams of composites with different contents of H ₄ TBAPy at different excitation wavelengths.....	6
Figure S12 a. Comparison of the fluorescence emission intensity of the Eu-MCTCA@H ₄ TBAPy-0.75 interacting with different metal ions under the same conditions b. Fluorescent intensity of different metal ions.....	7
Figure S13 Fitting of the Stern-Volmer plot of detecting Fe ³⁺	7
Figure S14 The competition experiments for the detection of Fe ³⁺ in the presence of different metal ions	8
Figure S15 a. Comparison of the luminescence intensity of the Eu-MCTCA@H ₄ TBAPy-0.75 interacting with different anions under the same conditions b. Fluorescent intensity of different anions.....	8
Figure S16 Fitting of the Stern-Volmer plot of detecting Cr ₂ O ₇ ²⁻	9
Figure S17 The competition experiments for the detection of Cr ₂ O ₇ ²⁻ in the presence of different anions	9

Figure S18	PXRD spectra of the Eu-MCTCA@H ₄ TBAPy before and after soaking in Fe ³⁺ , Cr ₂ O ₇ ²⁻ and colchicine solution in 24 h	9
Figure S19	UV-vis spectra of Fe ³⁺ , Cr ₂ O ₇ ²⁻ and colchicine and emission spectra of Eu-MCTCA@H ₄ TBAPy-0.75	10
Figure S20	Lifetime decay curve of composite Eu-MCTCA@H ₄ TBAPy	10
Figure S21	Fluorescence lifetime decay curve of composite Eu-MCTCA@H ₄ TBAPy-0.75 for detecting Fe ³⁺	10
Figure S22	Fluorescence lifetime decay curve of composite Eu-MCTCA@H ₄ TBAPy-0.75 for detecting Cr ₂ O ₇ ²⁻	11
Figure S23	Fluorescence lifetime decay curves of Eu-MCTCA for detecting colchicine	11
Figure S24	Fluorescence lifetime decay curves of composite Eu-MCTCA@H ₄ TBAPy-0.75 for detecting colchicine	12
Figure S25	UV-vis spectra of Fe ³⁺ , Cr ₂ O ₇ ²⁻ and colchicine and excitation spectra of Eu-MCTCA@H ₄ TBAPy-0.75	12
Figure S26	UV-vis spectrum H ₄ TBAPy	13
Figure S27	UV-vis spectra of Eu-MCTCA@H ₄ TBAPy, Fe ³⁺ , Cr ₂ O ₇ ²⁻ and colchicine	13
Table S1	CIE color coordinates of composites with different contents of H ₄ TBAPy at different excitation wavelengths	14
Table S2	Detection of fluorescence quenching rate constants for Fe ³⁺ ions by other materials*	14
Table S3	Detection of fluorescence quenching rate constants for Cr ₂ O ₇ ²⁻ ions by other materials*	15
Table S4	Fluorescence lifetime data of each stage before and after detection	15

Synthetic process of the ligand H₂MCTCA

P-aminobenzoic acid (13.72 g, 0.10 mol) was dissolved in concentrated hydrochloric acid solution and cool to 0 °C. Then dissolved sodium nitrite (6.90 g, 0.10 mol) with 30 mL H₂O and add the resulting solution to the above reaction system with stirring for 30 min at 0 °C. After filtration, sodium azide (6.50 g, 0.10 mol) soluble in 20 mL H₂O was added to the solution and continued to stir for 4 h. The white solid (M) was obtained by vacuum filtration. Add 0.60 g of metal sodium (0.60 g, 0.02 mol) to 20 mL cold anhydrous EtOH. The resulting solution was mixed with ethyl acetoacetate (1.62 g, 0.02 mol) and then the intermediate M (3.26 g, 0.02 mol) was added. After stirring for 1 h at 0 °C, heated and refluxed the mixture to completely dissolve precipitate. The pale yellow product was precipitated by adjusting the pH to 6. The H₂MCTCA (4.08 g) was obtained with a yield of 83.08% after filtration under reduced pressure and purification by recrystallization. ¹H-NMR (400 MHz, *d*₆-DMSO): δ 13.285 (s, 2H), 8.19 (d, J = 8.53 Hz, 2H), 7.80 (d, J = 8.66 Hz, 2H), 2.57 (s, 3H). ¹³C-NMR (101 MHz, *d*₆-DMSO): 166.8, 162.9, 139.6, 139.0, 137.3, 132.5, 131.1, 125.9, 125.9, 10.3. ESI-Q-TOF-HRMS ([C₁₁H₉N₃O₄Na(M+Na)]⁺): calcd m/z = 270.0491, found m/z = 270.0486.

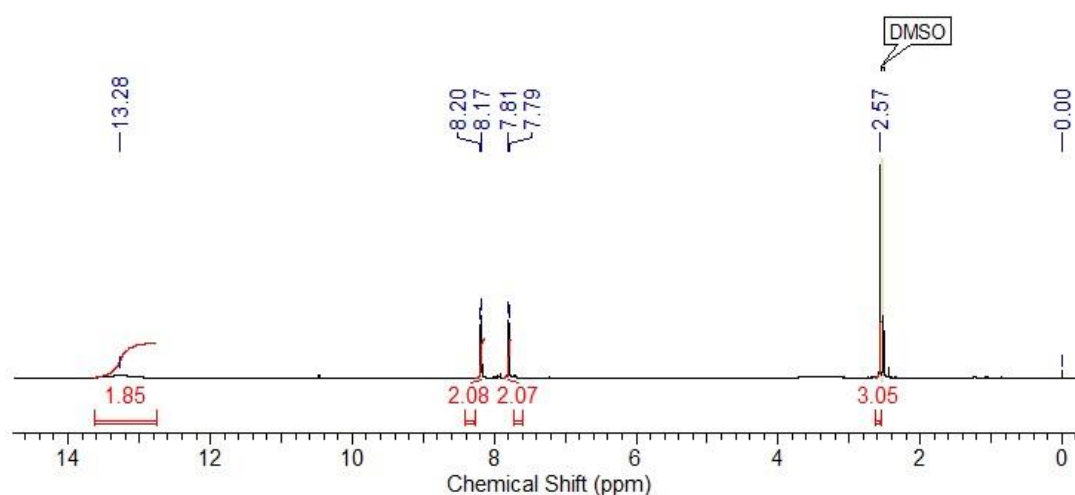


Figure S1. The ¹H-NMR spectrum of the ligand H₂MCTCA.

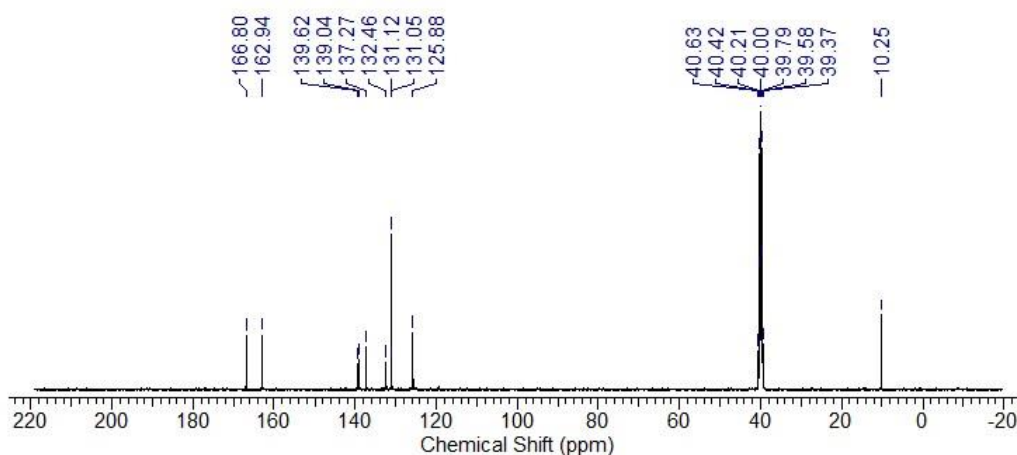


Figure S2. The ^{13}C -NMR spectrum of the ligand H_2MCTCA .

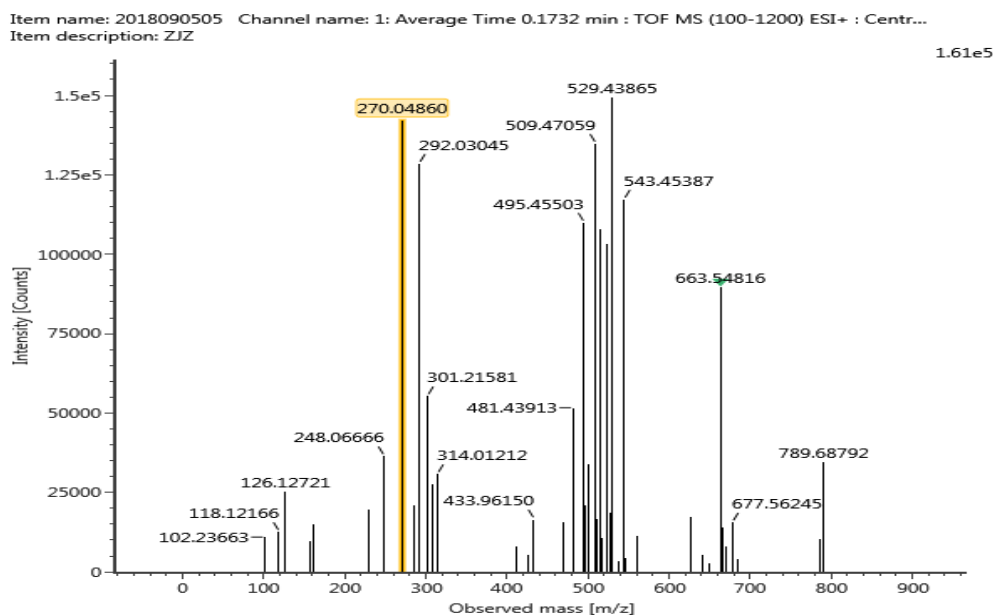


Figure S3. The HRMS spectrum of the ligand H_2MCTCA .

Synthetic process of the H_4TBAPy

Pyrene (10 g, 48 mmol), 300 mL of nitrobenzene, and excess bromine (11.2 mL, 218 mmol) were placed at 120 °C for 12 h. The product 1,3,6,8-tetrabromopyrene (M1) was filtered and washed by the solution of sodium hyposulfite (15%). A mixture of M1 (5 g, 9.5 mmol), (4-(methoxycarbonyl)-phenyl)boronic acid (8.5 g, 54.4 mmol), palladium tetrakis-(triphenylphosphine) (0.75 g 0.7 mmol), potassium

carbonate (16.5 g, 121 mmol), and dioxane (300 mL) was reacted for 3 day at 100 °C. The mixture was washed by water and acetone and extracted with chloroform (500 mL). Methanol (300 mL) was added and yellow precipitation occurred. 1,3,6,8-Tetrakis(4-(methoxycarbonyl)phenyl)pyrene (M2) was collected after filtration and then dried under vacuum. Then, KOH (7.1 g, 125.9 mmol), M2 (4.5 g, 6.1 mmol), and 1000 mL mixture of dioxane/H₂O (ratio 5/4) were refluxed for 18 h. The pH value was adjusted to 1 using concentrated hydrochloric acid (12 M) and yellow precipitation occurred. The product 1,3,6,8-tetrakis(pbenzoic acid)pyrene (H₄TBAPy, yellow solid) was collected, washed with water, recrystallized with mixed solution of DMF and dichloromethane, filtrated, and dried under vacuum for 36 h at 60 °C. It is named as H₄TBAPy. ¹H-NMR (400 MHz, DMSO-*d*₆, 298 K): δ 8.18 (s, 2H), 8.14 (d, J = 8.4 Hz, 4H), 8.05 (s, 1H), 7.82 (d, J = 8.4 Hz, 4H).

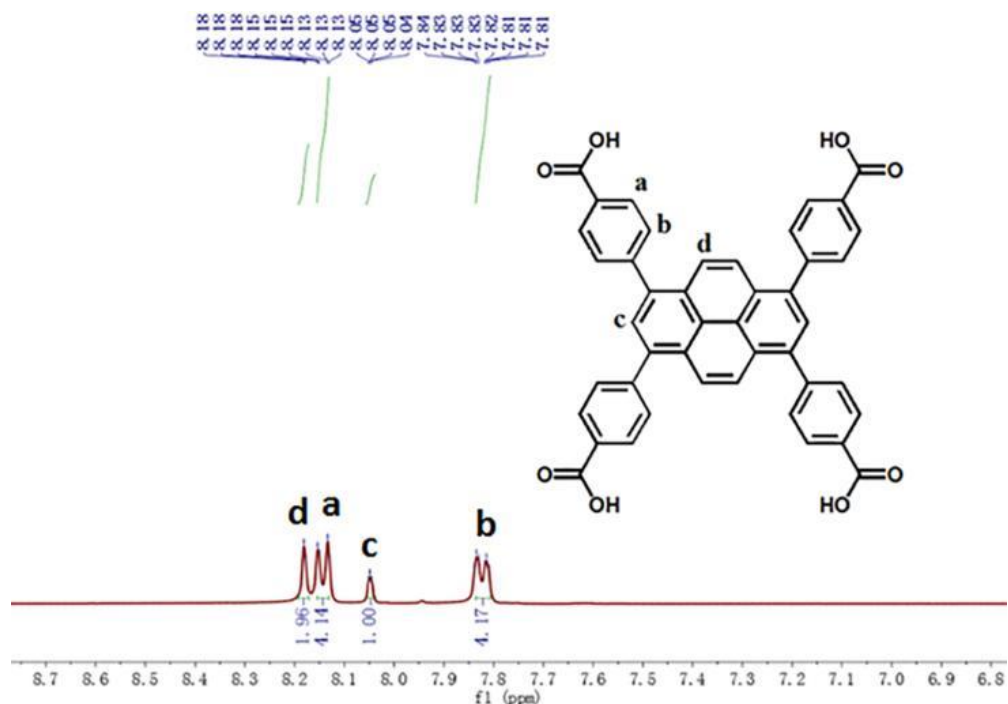


Figure S4. The ¹H-NMR spectrum of H₄TBAPy ligand in *d*₆-DMSO.

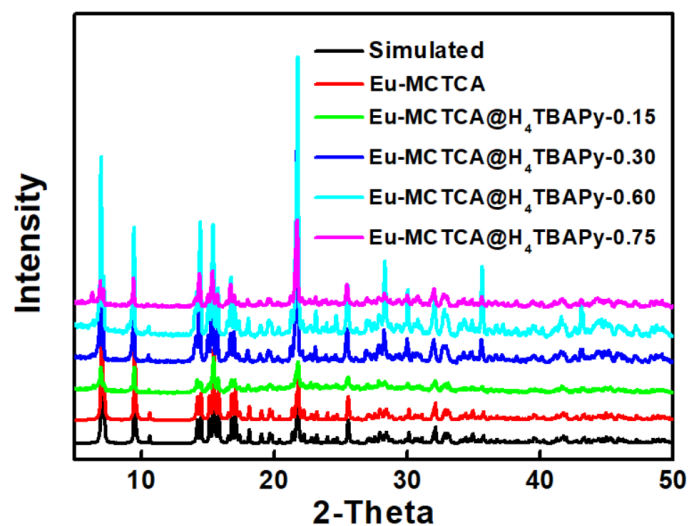


Figure S5 PXRD patterns of the Eu-MCTCA and Eu-MCTCA@H₄TBAPy.

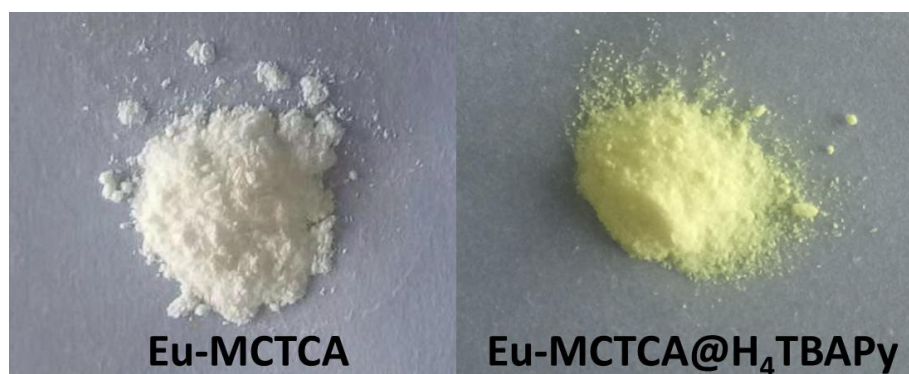


Figure S6 Appearance of Eu-MCTCA and Eu-MCTCA@H₄TBAPy.

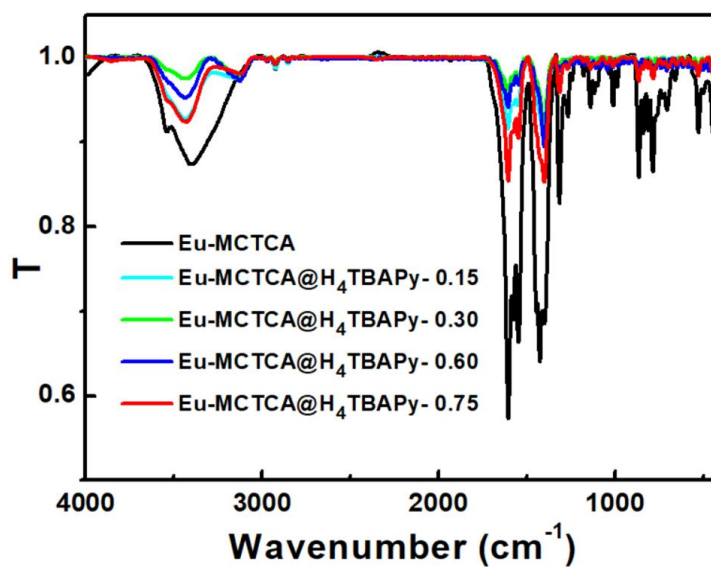


Figure S7 IR spectra of the Eu-MCTCA and Eu-MCTCA@H₄TBAPy.

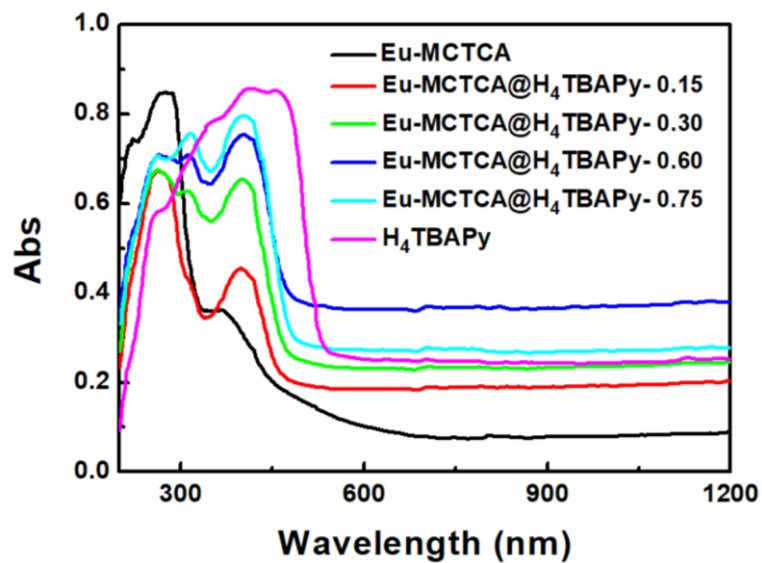


Figure S8 UV-vis spectra of the Eu-MCTCA and Eu-MCTCA@H₄TBAPy.

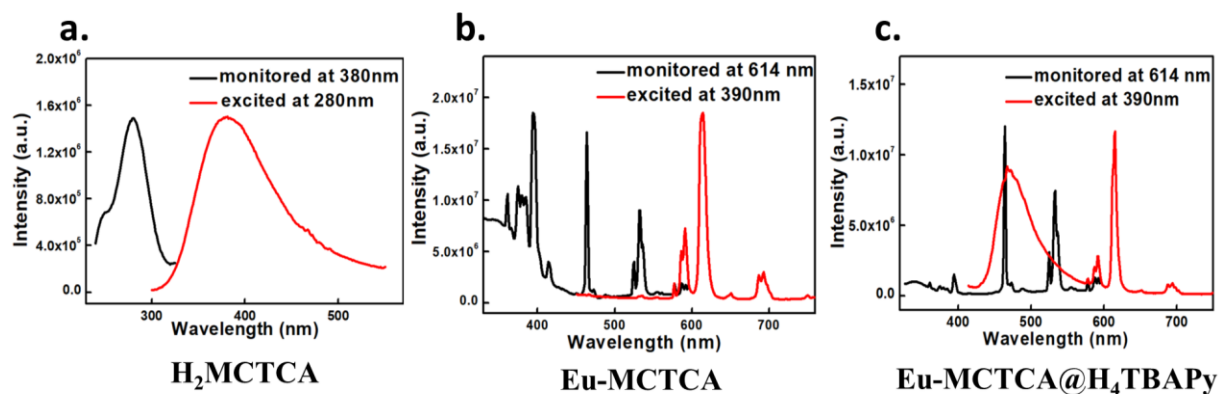


Figure S9 The solid-state luminescent spectra for H₂MCTCA(a) Eu-MCTCA(b) and Eu-MCTCA@H₄TBAPy(c) at room temperature.

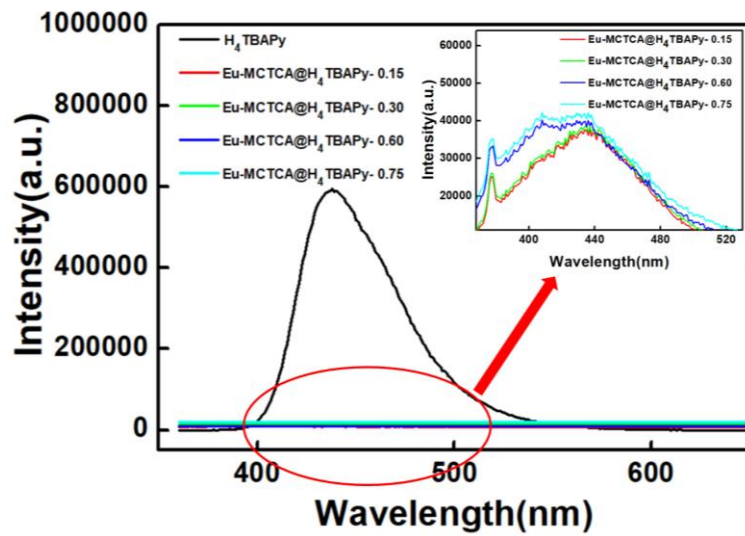


Figure S10 Fluorescence spectra of supernatant of H₄TBAPy and Eu-MCTCA@H₄TBAPy after ultrasonic treatment.

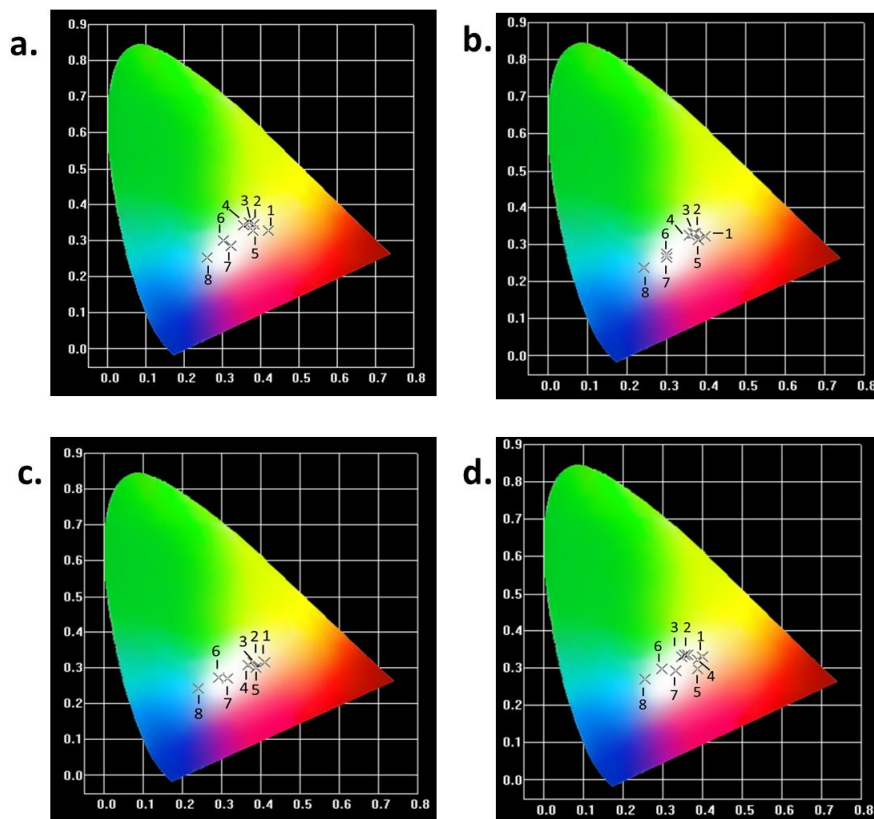


Figure S11 CIE chromaticity diagrams of composites with different contents of H₄TBAPy (**a.** 0.15 mM, **b.** 0.30 mM, **c.** 0.60 mM, **d.** 0.75 mM) at different excitation wavelengths (**1.** 320 nm, **2.** 330 nm, **3.** 340 nm, **4.** 350 nm, **5.** 360 nm, **6.** 370 nm, **7.** 380 nm, **8.** 390 nm).

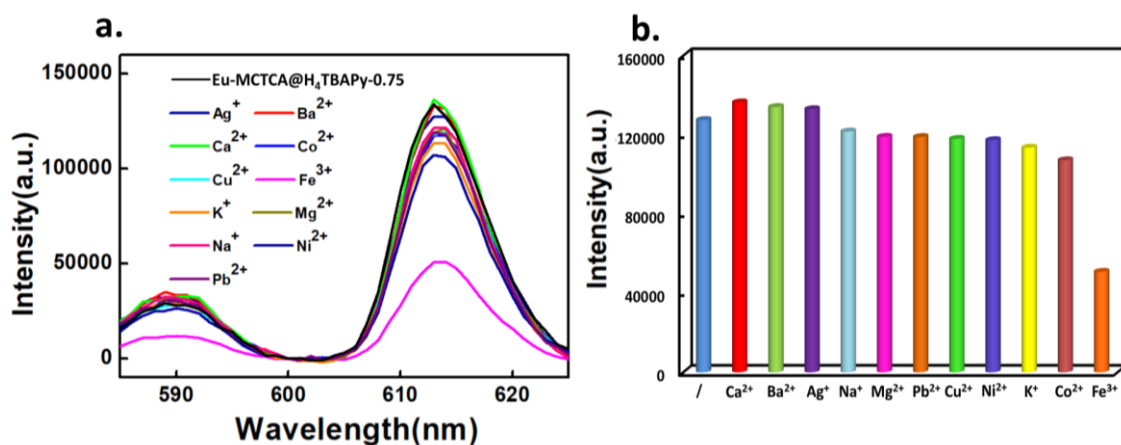


Figure S12 a. Comparison of the fluorescence emission intensity of the Eu-MCTCA@H₄TBAPy-0.75 interacting with different metal ions under the same conditions ($\lambda_{\text{ex}} = 360 \text{ nm}$) b. Fluorescent intensity of different metal ions.

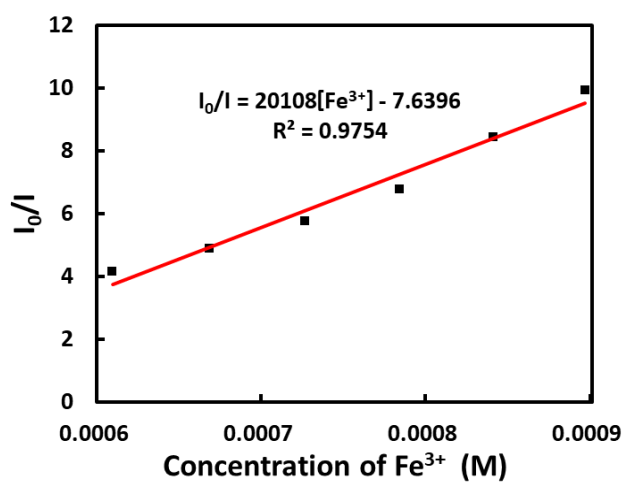


Figure S13 Fitting of the Stern-Volmer plot of detecting Fe³⁺.

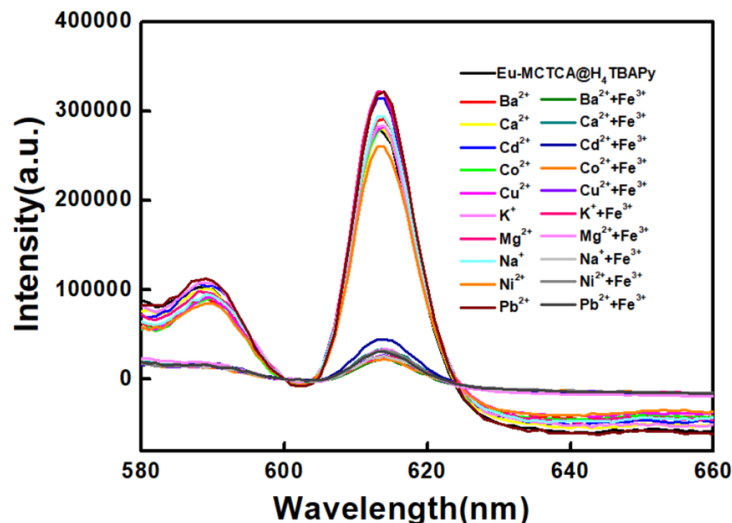


Figure S14 The competition experiments for the detection of Fe^{3+} in the presence of different metal ions.

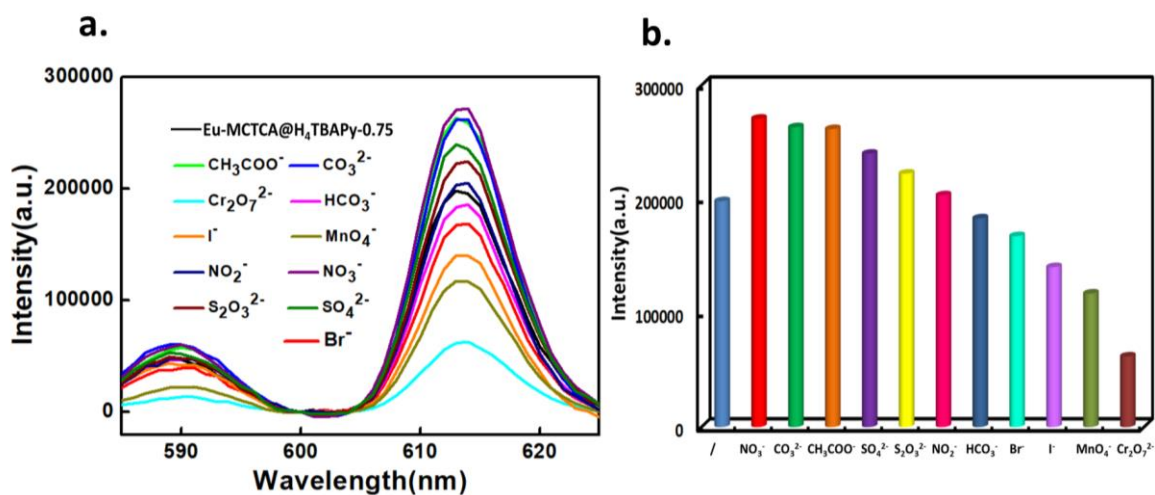


Figure S15 a. Comparison of the luminescence intensity of the Eu-MCTCA@H₄TBAPy-0.75 interacting with different anions under the same conditions ($\lambda_{\text{ex}} = 360 \text{ nm}$) b. Fluorescent intensity of different anions.

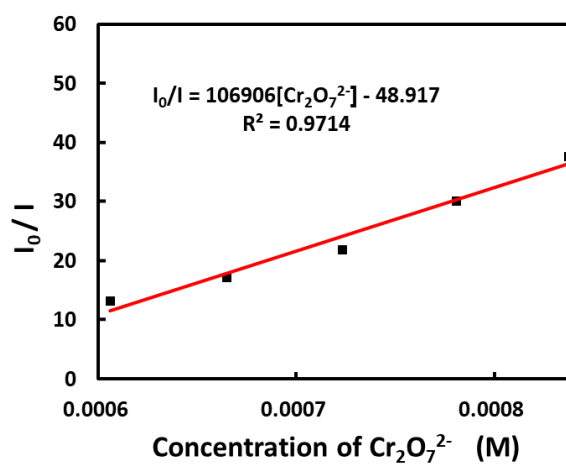


Figure S16 Fitting of the Stern-Volmer plot of detecting $\text{Cr}_2\text{O}_7^{2-}$.

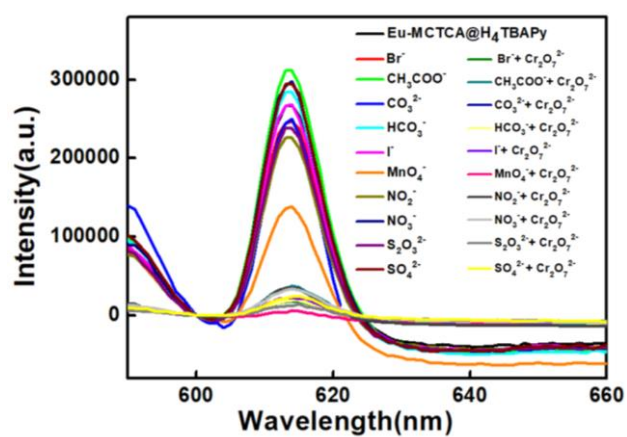


Figure S17 The competition experiments for the detection of $\text{Cr}_2\text{O}_7^{2-}$ in the presence of different anions.

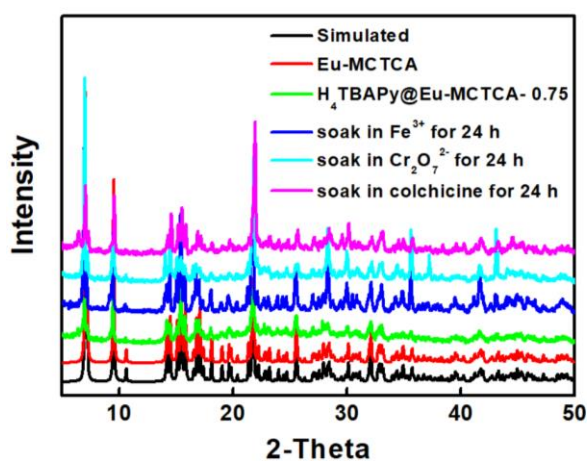


Figure S18 PXRD spectra of the Eu-MCTCA@ H_4TBAPy before and after soaking in Fe^{3+} , $\text{Cr}_2\text{O}_7^{2-}$ and colchicine solution in 24 h.

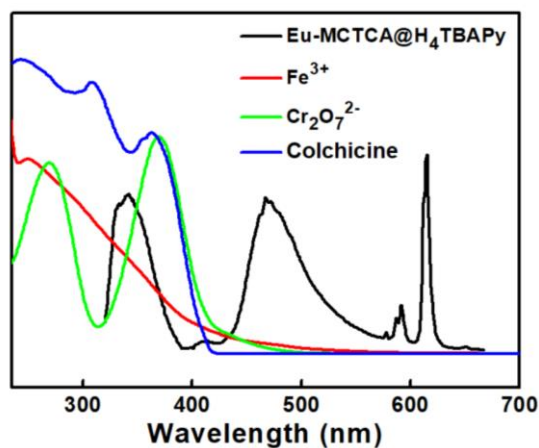


Figure S19 UV-vis spectra of Fe^{3+} , $\text{Cr}_2\text{O}_7^{2-}$ and colchicine and emission spectra of $\text{Eu-MCTCA@H}_4\text{TBAPy-0.75}$.

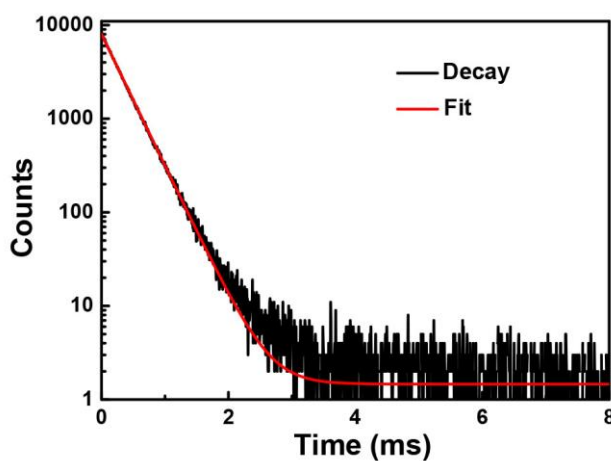


Figure S20 Lifetime decay curve of composite $\text{Eu-MCTCA@H}_4\text{TBAPy}$.

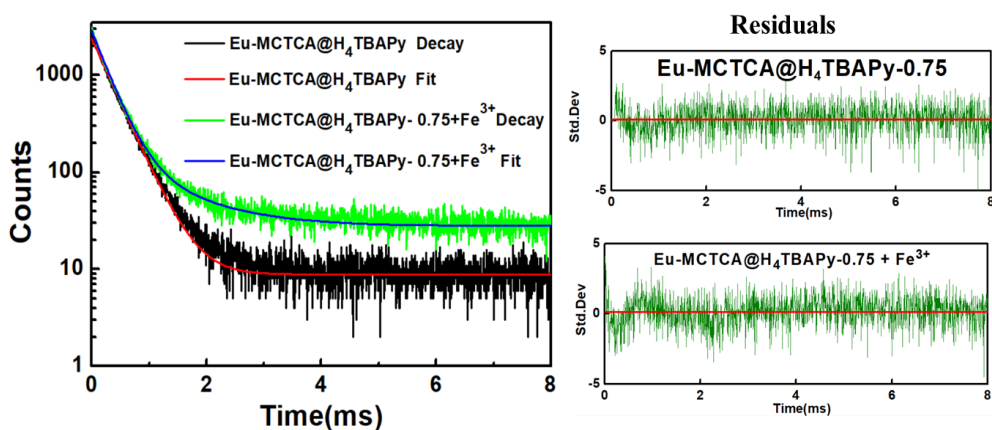


Figure S21 Fluorescence lifetime decay curve of composite $\text{Eu-MCTCA@H}_4\text{TBAPy-0.75}$ for detecting Fe^{3+} .

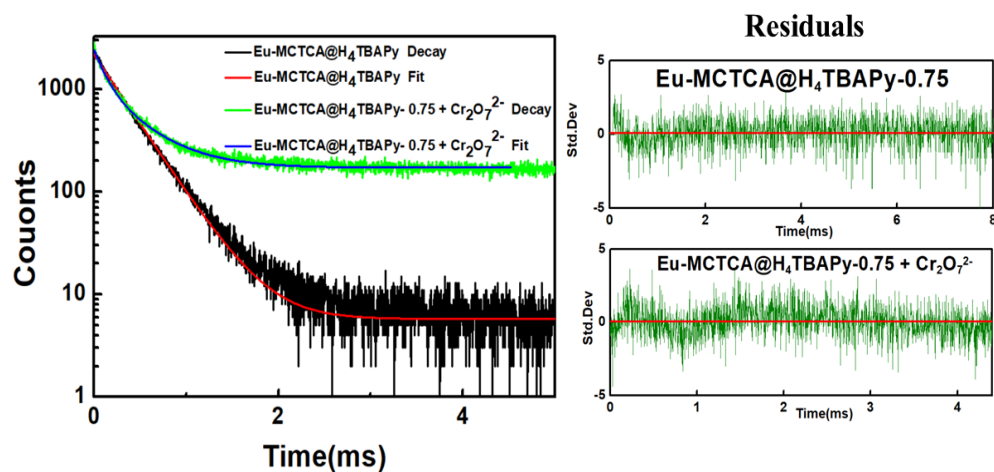


Figure S22 Fluorescence lifetime decay curve of composite Eu-MCTCA@H₄TBAPy-0.75 for detecting Cr₂O₇²⁻.

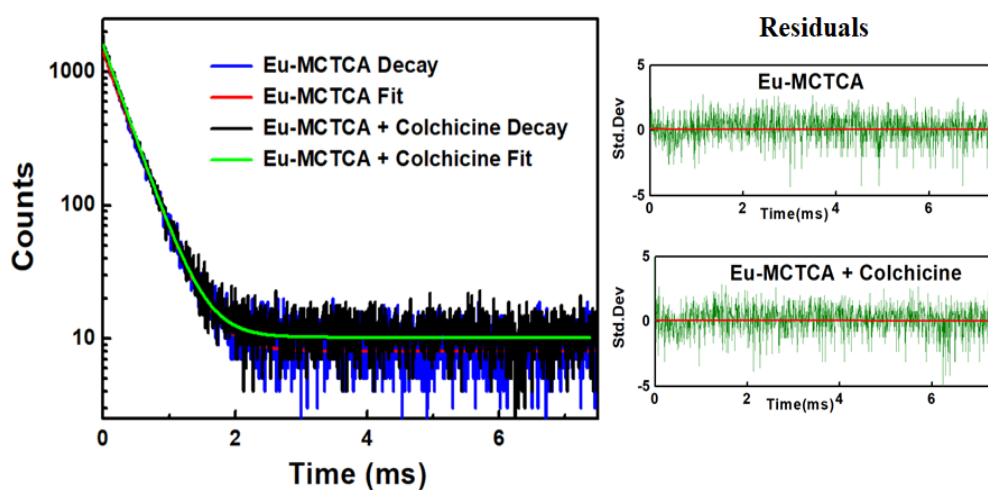


Figure S23 Fluorescence lifetime decay curves of Eu-MCTCA for detecting colchicine.

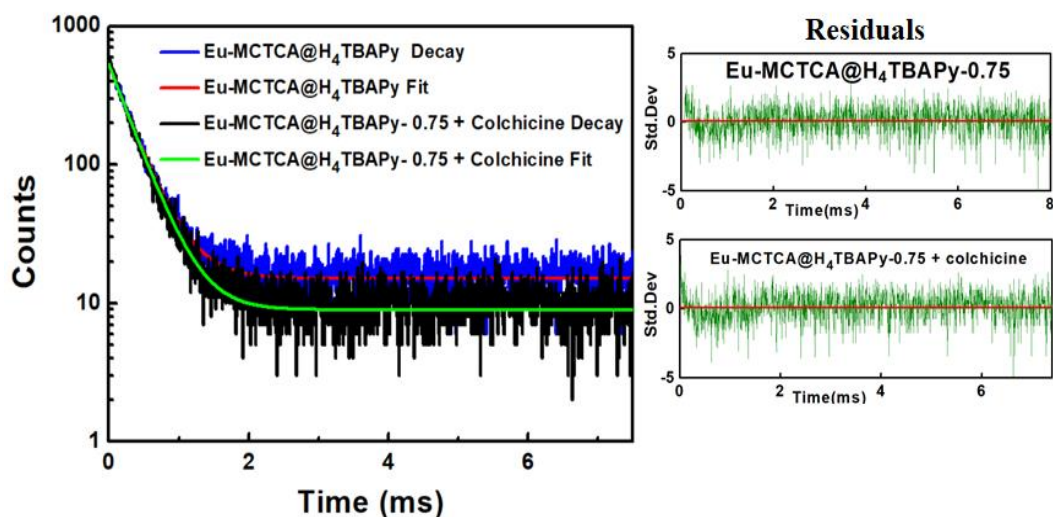


Figure S24 Fluorescence lifetime decay curves of composite Eu-MCTCA@H₄TBAPy-0.75 for detecting colchicine.

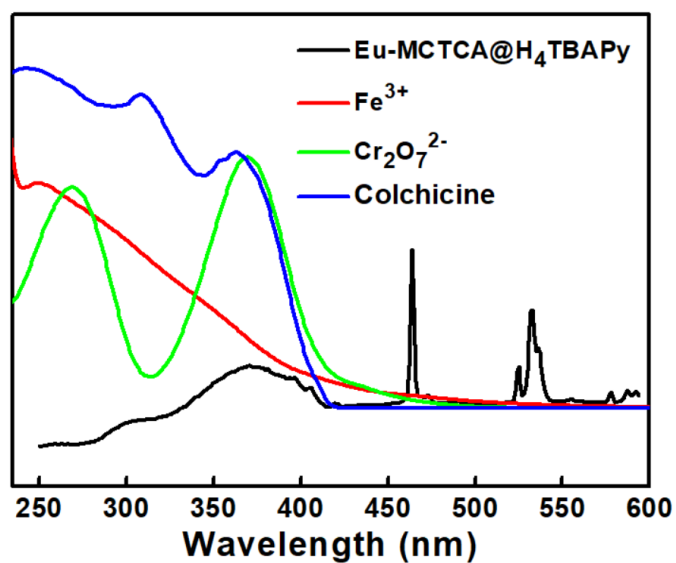


Figure S25 UV-vis spectra of Fe³⁺, Cr₂O₇²⁻ and colchicine and excitation spectra of Eu-MCTCA@H₄TBAPy-0.75.

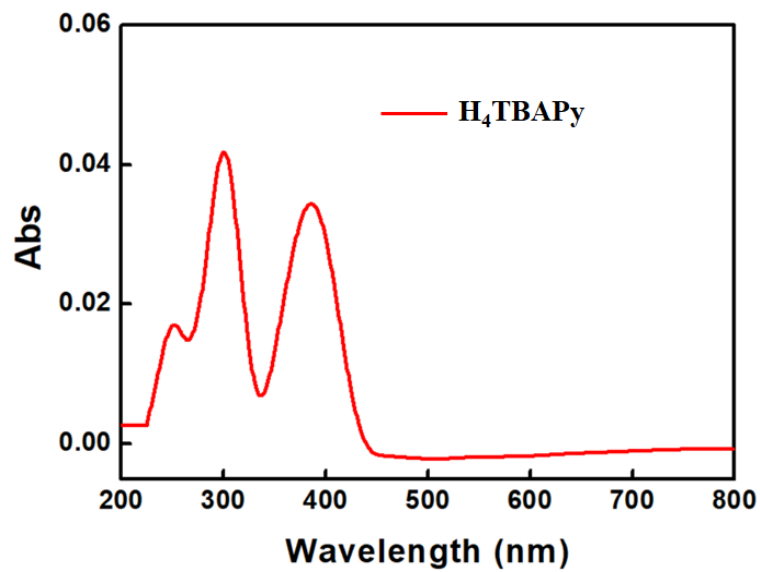


Figure S26 UV-vis spectrum H₄TBAPy.

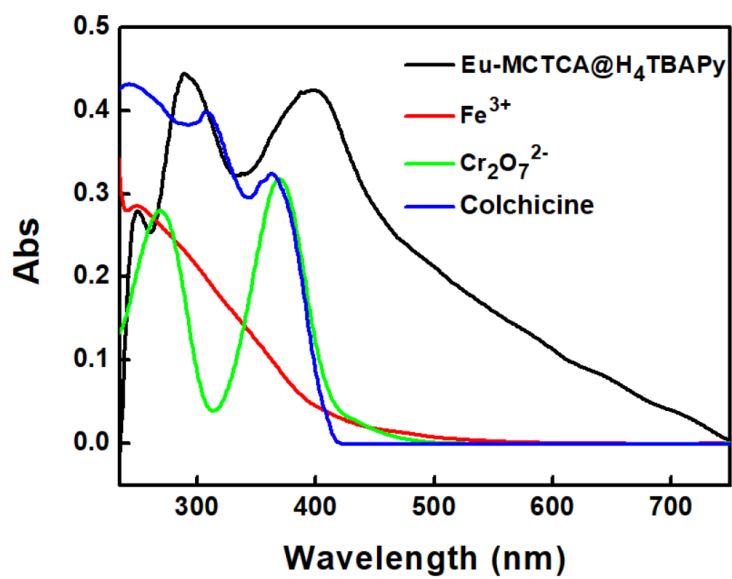


Figure S27 UV-vis spectra of Eu-MCTCA@H₄TBAPy, Fe³⁺, Cr₂O₇²⁻ and colchicine.

Table S1 CIE color coordinates of composites with different contents of H₄TBAPy(mM) at different excitation wavelengths.

	0.15	0.30	0.60	0.75
320nm	(0.4188, 0.3271)	(0.3986, 0.3238)	(0.4097, 0.3138)	(0.4001, 0.3299)
330nm	(0.3817, 0.3439)	(0.3718, 0.3304)	(0.3819, 0.3163)	(0.3615, 0.3345)
340nm	(0.3691, 0.3504)	(0.3677, 0.3308)	(0.3790, 0.3155)	(0.3557, 0.3357)
350nm	(0.3553, 0.3429)	(0.3582, 0.3248)	(0.3663, 0.3075)	(0.3482, 0.3301)
360nm	(0.3792, 0.3277)	(0.3800, 0.3122)	(0.3886, 0.3011)	(0.3885, 0.3228)
370nm	(0.3026, 0.3005)	(0.2992, 0.2753)	(0.2913, 0.2722)	(0.2980, 0.2980)
380nm	(0.3234, 0.2840)	(0.3142, 0.2646)	(0.3149, 0.2689)	(0.3331, 0.2932)
390nm	(0.2594, 0.2519)	(0.2420, 0.2373)	(0.2400, 0.2436)	(0.2555, 0.2707)

Table S2 Detection of fluorescence quenching rate constants for Fe³⁺ ions by other materials*

	Materials	K _{sv} (M ⁻¹)	References
1)	[Tb(L)(DMA)]·(DMA)·(0.5H ₂ O)	1.91×10 ³	[1]
2)	[Eu(IMS1) ₂]Cl·4H ₂ O	5.87×10 ³	[2]
3)	[La(TPT)(DMSO) ₂]·H ₂ O	1.36×10 ⁴	[3]
4)	Eu ³⁺ @MIL-53-COOH (Al)	5.12×10 ³	[4]
5)	EuL ₃	4.10×10 ³	[5]
6)	Tb-DSOA	3.54×10 ³	[6]
7)	Eu(atpt) _{1.5} (phen)(H ₂ O)	7.60×10 ³	[7]

*1) H₃L = 3'-hydroxybiphenyl-3,4',5-tricarboxylic acid;

2) IMS1 = 1,3-bis(4-carboxylbenzyl)-imidazolium;

3) H₃TPT = p-terphenyl-3,4'',5-tricarboxylate acid;

4) L = 4'-(4-carboxyphenyl)-2,2': 6',2''-terpyridine;

5) Na₂H₂DSOA = disodium-2,2'-disulfonate-4,4'-oxydibenzoic acid;

6) H₂atpt = 2-aminoterephthalic acid, phen=1,10-phenanthroline.

Table S3 Detection of fluorescence quenching rate constants
for $\text{Cr}_2\text{O}_7^{2-}$ ions by other materials*

	Materials	$K_{SV}(\text{M}^{-1})$	References
1)	$[\text{Eu}_2(\text{H}_2\text{O})(\text{DCPA})_3]_n$	8.7×10^3	[8]
2)	$\text{Eu}^{3+} @ \text{MIL-124}$	6.0×10^2	[9]
3)	$[\text{Eu}(\text{Hpzbc})_2(\text{NO}_3)] \text{H}_2\text{O}$	2.6×10^3	[10]
4)	$\text{Eu}^{3+} @ \text{MIL-121}$	4.34×10^3	[11]
5)	$\text{Tb}(\text{TBOT})(\text{H}_2\text{O})[(\text{H}_2\text{O})_4(\text{DMF})(\text{NMP})_{0.5}]$	1.37×10^4	[12]

* 1) H_2DCPA = 4,5-Dichlorophthalic acid;

2) MIL-124 = $\text{Ga}_2(\text{OH})_4(\text{C}_9\text{O}_6\text{H}_4)$, 2- NH_2bdc = 2-amino-1,4-benzene dicarboxylate;

3) Hpzbc = 3-(1H-pyrazol-3-yl) benzoate;

4) MIL-121 = $\text{Al}(\text{OH})(\text{H}_2\text{btec}) \text{H}_2\text{O}$;

5) TBOT = 2,4,6-tris[1-(3-carboxylphenoxy)ylmethyl]mesitylene, NMP = N-methyl-2-pyrrolidone.

Table S4 Emission lifetime data of the lifetime of each stage
before and after detection.

	τ_1 [amplitude](ms)	τ_2 [amplitude] (ms)	τ_{ave} (ms)
Eu-MCTCA@ H_4TBAPy	0.3265443[1.0]	-	0.3265443
Eu-MCTCA@ $\text{H}_4\text{TBAPy} + \text{Fe}^{3+}$	0.2769756[0.83]	1.123915[0.16]	0.3170616
Eu-MCTCA@ $\text{H}_4\text{TBAPy} + \text{Cr}_2\text{O}_7^{2-}$	0.1231029[0.27]	0.4406017[0.73]	0.2599026
Eu-MCTCA@ $\text{H}_4\text{TBAPy} + \text{colchicine}$	0.3205254[1.0]	-	0.3205254
Eu-MCTCA	0.3185820[1.0]	-	0.3185820
Eu-MCTCA+colchicine	0.3059430[1.0]	-	0.3059430

References

1. S. Pal, P. K. Bharadwaj, *Cryst Growth Des.*, 2016, **16**, 5852-5858.
2. Y. Q. Huang, H. Y. Chen, Y. Wang, *RSC Advances.*, 2018, **8**, 21444-21450.
3. C. Q. Zhang, Y. Yan, Q. H. Pan, *Dalton T.*, 2015, **44**, 13340-13346.
4. Y. Zhou, H. H. Chen, B. Yan, *J. Mater. Chem. A.*, 2014, **2**, 13691-13697.
5. M. Zheng, H. Q. Tan, Z. G. Xie, *ACS Appl. Mater. Inter.*, 2013, **5**, 1078-1083.
6. X. Y. Dong, R. Wang, J. Z. Wang, *J. Mater. Chem. A.*, 2015, **3**, 641-647.
7. Y. Kang, X. J. Zheng, L. P. Jin, *J. Colloid. Interf. Sci.*, 2016, **471**, 1-6.
8. H. M. He, S. H. Chen, D. Y. Zhang, R. Hao, C. Zhang, E. C. Yang, X. J. Zhao, *Dalton Trans.*, 2017, **46**, 13502-13509.
9. X.Y. Xu, B. Yan, *ACS Appl. Mater. Inter.*, 2015, **7**, 721-729.
10. G.P. Li, G. Liu, Y.Z. Li, L. Hou, Y.Y. Wang and Z. H. Zhu, *Inorg. Chem.*, 2016, **55**, 3952-3959.
11. J.N. Hao, B. Yan, *New J Chem.*, 2016, **40**, 4654-4661.
12. M. Chen, W.M. Xu, J.Y. Tian, H. Cui, J.X. Zhang, C.S. Liu and M. Du, *J. Mater. Chem. C.*, 2017, **5**, 2015-1021.